

Cell-based simulation of dynamic expression patterns in the presomitic mesoderm

Hendrik B. Tiedemann^a, Elida Schneltzer^a, Stefan Zeiser^b, Isabel Rubio-Aliaga^a,
Wolfgang Wurst^c, Johannes Beckers^a, Gerhard K.H. Przemeck^a, Martin Hrabé de Angelis^{a,*}

^a*Institute of Experimental Genetics, GSF-National Research Centre for Environment and Health, Ingolstädter Landstraße 1, D-85764 Neuherberg, Germany*

^b*Institute of Biomathematics and Biometry, GSF-National Research Centre for Environment and Health, Ingolstädter Landstraße 1, D-85764 Neuherberg, Germany*

^c*Institute of Developmental Genetics, GSF-National Research Centre for Environment and Health, Ingolstädter Landstraße 1, D-85764 Neuherberg, Germany*

Received 24 October 2006; received in revised form 4 April 2007; accepted 14 May 2007

Available online 21 May 2007

Abstract

To model dynamic expression patterns in somitogenesis we developed a Java-application for simulating gene regulatory networks in many cells in parallel and visualising the results using the Java3D API, thus simulating the collective behaviour of many thousand cells. According to the ‘clock-and-wave-front’ model mesodermal segmentation of vertebrate embryos is regulated by a ‘segmentation clock’, which oscillates with a period of about 2 h in mice, and a ‘wave front’ moving back with the growing caudal end of the presomitic mesoderm. The clock is realised through cycling expression of genes such as *Hes1* and *Hes7*, whose gene products repress the transcription of their encoding genes in a negative feedback loop. By coupling the decay of the *Hes1* mRNA to a gradient with the same features and mechanism of formation as the mesodermal *Fgf8* gradient we can simulate typical features of the dynamic expression pattern of *Hes1* in the presomitic mesoderm. Furthermore, our program is able to synchronise *Hes1* oscillations in thousands of cells through simulated Delta–Notch signalling interactions.

© 2007 Elsevier Ltd. All rights reserved.

Keywords: Somitogenesis; Object-oriented modelling; *Hes1*; *Fgf8* gradient; Delta–Notch signalling

1. Introduction

The segmentation of the adult vertebrate body is evident for example in the reiterated structures of the vertebrate axial skeleton, spinal nervous system and body muscles. It is established in embryogenesis after gastrulation when at the rostral end of the presomitic mesoderm (PSM) on both sides of the neural tube segments termed somites separate from the PSM. In these somites the outer cells change their tissue type from mesodermal to epithelial. Later the somitic cells change their adhesive and migratory properties, and finally contribute to the adult structures mentioned above. Somites are generated successively, one pair after the other, from the PSM. Waves of gene expression starting at the posterior tip of the PSM and running in anterior direction

are leading to the formation of one somite at the anterior end of the PSM at both sides of the neural tube for each upcoming ‘wave’ (Dale and Pourquie, 2000; Saga and Takeda, 2001).

The first of this ‘cycling genes’ was discovered in the development of the chick. It was shown (Palmeirim et al., 1997) by in situ hybridisation that the *Hairy1* gene shows a periodically repeating expression pattern. It starts with a strong expression at the caudal end, extends then rostrally, while weakening at the tail, and finally contracts into a narrow stripe. This anterior stripe of expression marks the region where the next somite will form. Interestingly, experimental manipulation in chick showed that this ‘wave’ of gene expression could not even be stopped by cutting out a wedge of the middle PSM (Palmeirim et al., 1997), which gives rise to the question how the ‘wave’ can bridge this gap in mesodermal tissue. This experiment argues against a mechanism based on the diffusion of signalling

*Corresponding author. Tel.: +49 89 3187 3302; fax: +49 89 3187 3500.
E-mail address: hrabe@gsf.de (M. Hrabé de Angelis).

molecules. A similar expression pattern for the orthologous gene *Hes1* was found in mice (Jouve et al., 2000). Later, it was discovered that *Hes1* is not only expressed in the PSM but in many other tissues as well. Another member of the Hes-family of bHLH-proteins, *Hes7*, was identified (Bessho et al., 2001a, b). It is restricted to the PSM and the corresponding mRNA displays a similar expression pattern as *Hes1*. However, only *Hes1* could be studied in cell culture. Cultured fibroblast cells were induced to express the gene in an oscillatory manner (Hirata et al., 2002). It was shown that *Hes1* represses its own transcription by binding as homo-dimers to three so-called N-boxes in its promoter (Takebayashi et al., 1994). The half-life times of the *Hes1* mRNA and protein were measured. These data allowed a differential equation model to be built for mRNA, protein and a postulated factor, termed Z, which exhibited oscillatory behaviour with the expected period of roughly 2 h (Hirata et al., 2002).

Later, Monk could describe these oscillations without the Z-factor by using delay differential equations (Monk, 2003). The same was accomplished in the zebrafish system for the *her1* and *her7* genes (Lewis, 2003). Lower bounds for the delays were estimated from the length of the genes and proteins by using the known polymerisation rates of RNA-polymerase II and ribosome, respectively (Lewis, 2003). This model was also used to describe the *Hes7* oscillations in mouse and its abolishment observed in mouse embryos expressing mutant *Hes7* protein with a longer half-life (Hirata et al., 2004).

It is now generally believed that the cycling genes represent the clock part of the ‘clock- and wave-front’ model formulated by Cooke and Zeeman (1976). The ‘wave-front’, which moves backward with the caudal end and determines where new somites are formed in the PSM, could possibly be explained by the *Fgf8* gradient discovered recently in the PSM of mice (Dubrulle and Pourquie, 2004a, b). This gradient is not generated by diffusion, but by the constant growth of the PSM and the continuous transcription of *Fgf8* in the growing tail-bud, while transcription ceases in the rest of the PSM. The *Fgf8* mRNA decays with a comparatively long half-life of the order of hours (Dubrulle and Pourquie, 2004a). It is translated into protein in the entire PSM—not only the growth zone—leading to a graded distribution of mRNA and protein along the rostro-caudal axis of the PSM.

Here we present a computer model to explain the dynamic gene expression patterns in somitogenesis and the collective behaviour of many cells. The model is cell based with a gene regulatory network inside each cell described by differential equations. The cells can proliferate and display the concentration of a user-selected mRNA or protein by the intensity of their colouration. As a first step we try to understand the dynamics of *Hes1* expression in the tail-bud phase when a group of stem cells provides for a roughly constant length of the PSM while new somites separate from the anterior end of the PSM (Brown et al., 2006; Dale and Pourquie, 2000; Deschamps and van

Nes, 2005). When we incorporated the *Fgf8* gradient described above in our computer model of the growing PSM and coupled the gradient linearly to various models of the *Hes1* oscillator in each cell, we observed the characteristic ‘wave’ progressing from posterior to anterior PSM, narrowing while moving forward, and coming to a stop finally. This process repeats itself as long as the PSM is growing, forming the characteristic stripe pattern for the *Hes1* mRNA expression.

The cycling genes are mostly part or effectors of the Delta–Notch signalling pathway. Disturbing this pathway leads to a disruption of somitogenesis (Hrabe de Angelis et al., 1997), probably because the direct cell to cell signalling synchronises the oscillations in neighbouring cells and stabilises the expression patterns against fluctuations (Jiang et al., 2000). Therefore, as a next step, we gave our virtual cells the ability to recognise nearest neighbours and synchronise their oscillations by Delta–Notch signalling.

2. Methods

To simulate the dynamics of the mRNA expression during somitogenesis we developed a program written in the Java language using the Java3D API.

As somitogenesis is a dynamic phenomenon which involves cell proliferation, waves of gene expression, cell polarisation, etc., a data structure was needed to model this collective behaviour of many cells. In addition, visualisation of cell behaviour and gene expression had to be integrated. Therefore object-oriented modelling was employed: A cell is described as an instance of a Java object with methods for cell division, cell death, propagating in time the concentration variables of the gene regulatory network inside the cell, and displaying concentration of protein or mRNA as intensity of colouration of each cell (virtual in situ staining). To shorten rendering time each cell is displayed as a sphere or symmetrical polyhedron. Furthermore, the simulated cells are able to recognise their nearest neighbours. Internal variables describing Delta–Notch pairs are created accordingly and integrated into the reaction network. Cell division and death are modelled phenomenologically, i.e. purely descriptive, and provide the ‘boundary conditions’ for processes that are simulated by more detailed models (e.g. reaction networks). For example, cell proliferation is modelled by a process which creates a copy of the ‘mother cell’ furnished with the equivalent variables for the gene regulatory network. The ‘daughter cell’ ‘grows’ out of the ‘mother cell’ along a fixed direction. This growth stops when both cells are separated. The ‘daughter cell’ then develops as an autonomous unit.

Of course, it is currently not possible to describe all the thousands of polymerisation reactions (for the generation of the mRNA and its translation into protein) and the numerous processing steps of the mRNAs in detail. To simulate the biochemical reactions we employed a kinetic equation framework with differential equations for the temporal development of the variables describing mRNA

and describes the negative feedback of the *Hes1* protein on the *Hes1* mRNA. We have chosen Hill-coefficient $h = 3$, i.e. strong cooperativity between the *Hes1* dimers (Zeiser et al., in press), and Hill-constant $H = 1.0$.

The gradient is given by two equations for *Fgf8* mRNA and protein. We do not distinguish between nucleus and cytoplasm here because of the long decay time of the mRNA (Dubrulle and Pourquie, 2004a) which implies that the dynamics of *Fgf8* is comparatively slow:

$$\begin{aligned}\frac{dm_{Fgf8}(t)}{dt} &= K_{growth} f_h(p_{Fgf8}(t)) - am_{Fgf8}(t), \\ \frac{dp_{Fgf8}(t)}{dt} &= bm_{Fgf8}(t) - cp_{Fgf8}(t).\end{aligned}\quad (3)$$

Fgf8 protein and mRNA decay rates are given by $c = 0.03$ and $a = 0.006$, respectively, which are inversely proportional to the respective protein and mRNA half-lives τ_p and τ_m : $c = \ln 2/\tau_p$, $a = \ln 2/\tau_m$. For the *Fgf8* mRNA half-life we adopt a value circa 2 h, as in Dubrulle and Pourquie (2004a) it was only estimated to be several hours. For lack of data we assumed a half-life of 20 min for the *Fgf8* protein. The other constants were chosen so that a constant *Fgf8* protein concentration was obtained in the growth zone, where *Fgf8* mRNA expression is active. So for cells in the growth zone the program sets $K_{growth} = 54.702$. When a cell is not part of the growth zone any more, K_{growth} is set to zero. The mRNA then simply decays exponentially. As we do not know by which processes *Fgf8* itself is regulated, we held the concentrations of mRNA and protein constant in the growth zone by employing a simple negative feedback loop with a Hill-coefficient of 2 and a Hill-constant of 1. For *Fgf8* the translation rate is set to $b = 0.3$.

The *Hes1* oscillator and the *Fgf8* gradient are coupled by multiplying the *Hes1* mRNA decay term D with the concentration of *Fgf8* protein—normalised to 1 in the growth zone—still remaining in the respective cell of the PSM. The normalisation ensures that the *Fgf8* mRNA and protein concentration in the growth zone can be chosen arbitrarily as long as we do not know more about the nature of the coupling of the gradient to the *Hes1* mRNA decay.

3. Results

3.1. Wave-like gene expression patterns

With our program we simulated several models for the time course of *Hes1* expression in the growing PSM in the tail-bud phase, each differing in the choice of kinetic equations describing the *Hes1* oscillations in one cell:

We began with the original model devised by Hirata et al. (2002) which has the disadvantage that an unknown factor termed Z had to be introduced to get a delay causing the oscillations. When Monk (2003) and Lewis (2003) formulated the oscillator model with only two delay differential equations for mRNA and protein we

incorporated this model in our program also. However, delay differential equations pose mathematical difficulties. So we developed a two-compartment (nucleus and cytoplasm) transport model in two variants instead. The first (model 1) regards two compartments only for the *Hes1* protein while the second (model 2) also describes in addition the transport of the *Hes1* mRNA from nucleus to cytoplasm.

Using the measured decay rates for the *Hes1* protein, *Hes1* mRNA (Hirata et al., 2002), and *Fgf8* mRNA (Dubrulle and Pourquie, 2004a) we were able to reproduce the dynamic pattern of an expression wave moving from the caudal to the rostral end of the PSM. Similar to *Hes1* expression in mouse embryos the progressing wave narrowed and finally came to a stop at the anterior end of the PSM. (However, it can take several oscillation cycles, until a stripe settles in its final position, as small movements of the stripe of one or two cell diameters can happen occasionally after the stripe halted for the first time.) Fig. 2 shows three stages of an oscillation cycle in situ and for our model 1, which we will discuss in more detail in the following. The other models show qualitatively similar expression patterns, except that the width, intensity and stability of the resulting stripe pattern were different (supplementary information).

One should emphasise that in our model the expression wave is only an apparent wave, which appears to an observer because the oscillations in an individual cell slow down ever more as the growth zone moves away from it. This is shown in Fig. 3 for two cells: one which ends up with a high final mRNA concentration, i.e. will form part of a stripe in the pattern, the other with a lower final concentration value in an inter-stripe region. Both cells are born at different times and therefore enter the gradient while being in different phases of their oscillations. However, in Fig. 3 both curves start at time zero because the time on the abscissa is the lifetime of each cell. The concentration data were written to file during a simulation run.

The *Hes1* protein decay is effected by ubiquitination and processing in the proteasomes (Hirata et al., 2002), which are located in the cytoplasm as well as in the nucleus (Rivett, 1998; Muratani and Tansey, 2003). Describing *Hes1* decay assuming different kinetic equations in nucleus and cytoplasm which allow for a possible saturation of the proteasome machinery in the cell nucleus while disregarding this possibility in the cytoplasm, one gets a stable stripe expression pattern rostrally to the wave zone (movie1). If, however, one assumes a linear concentration dependence of protein decay everywhere, the stripe pattern is unstable in the sense that the low expression regions fill up slowly (data not shown). The same happens in the case of Lewis' oscillator model for zebrafish (Lewis, 2003) (movie5) and the model formulated for *Hes7* (Monk, 2003; Hirata et al., 2004). If one uses the old model of Hirata et al. (2002), coupling the *Fgf8* gradient to the decay of the *Hes1* mRNA and the decay of the Z -factor, a stable stripe pattern forms,

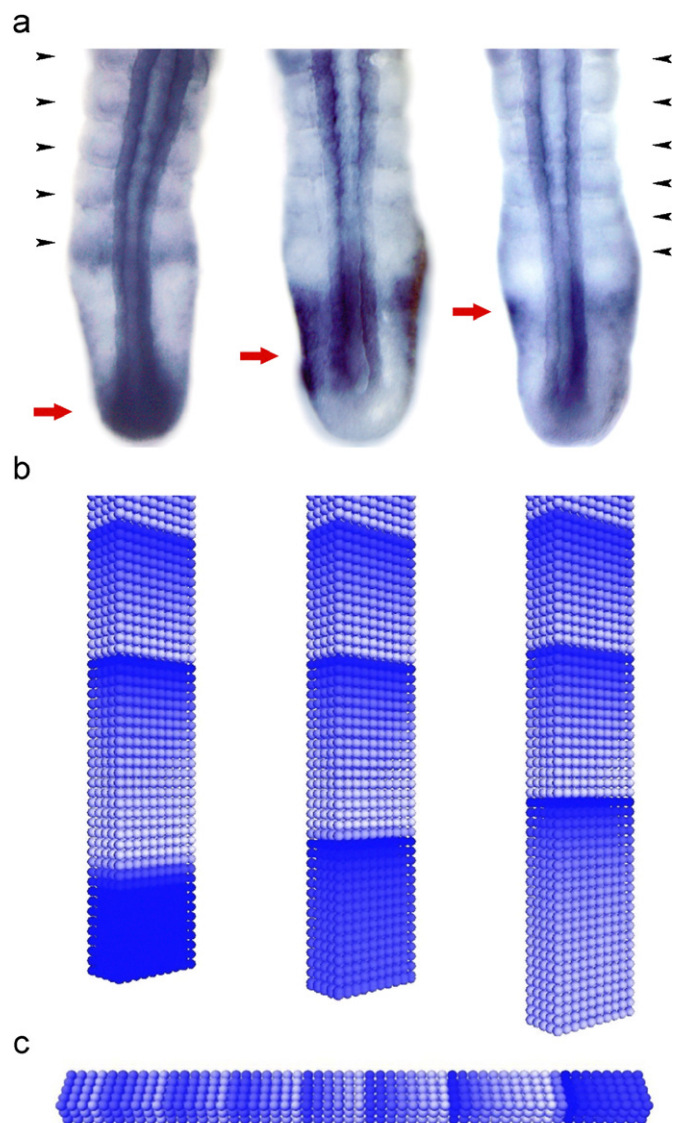


Fig. 2. Picture of in situ hybridisation of *Hes1* mRNA in the murine presomitic mesoderm (PSM) at day E10.5 (a), snapshots of the simulation of the growing PSM with the concentration of *Hes1* mRNA indicated by colour intensity (b), and a simulation with the growth rate of the PSM halved (c).

but the expression stripes are narrower than in the model proposed here (movie4).

The results for our model 1 are rather insensitive to a variation of the *Fgf8* mRNA half-life. A doubling of the half-life to 4 h (movie2) or a reduction to 30 min (movie3) resulted in a stripe pattern with almost the same spacing between stripes. However, cells oscillate 6 times or 1.5 times, respectively, before reaching a stationary state. The ‘wave zone’ of the PSM is lengthened or shortened accordingly, although not proportionally (data not shown).

Also varying the Hill-coefficient for the cellular oscillators in the range between 3.0 and 2.0 (3.0, 2.7, 2.4, 2.0) does not change the behaviour described above. Here a Hill-coefficient of 2.4 describes the binding of three very weakly interacting *Hes1* dimers to the three N-boxes, while

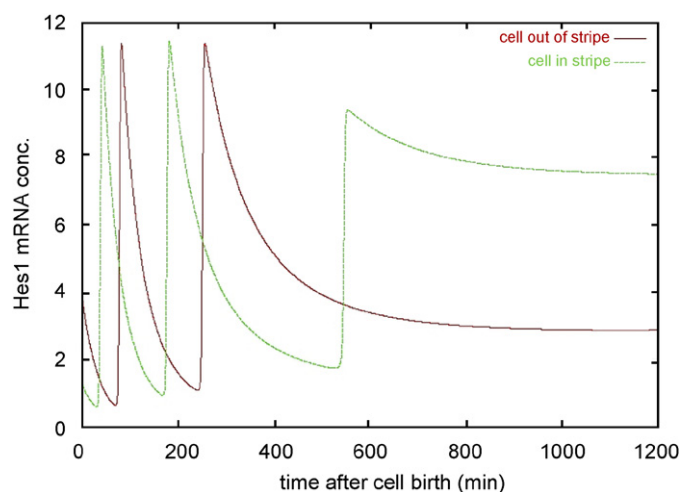


Fig. 3. Plot of the oscillations of *Hes1* mRNA concentration for a cell which ends up in stripe and for a cell in an inter-stripe region.

a value of 2 is appropriate in the case of one dimer regulating its corresponding gene (Zeiser et al., in press). As the only effects of a reduction of the Hill-coefficient we found a reduction of the maximal *Hes1* mRNA concentration of about 20% and a diminished difference in expression between stripe- and inter-stripe cells (data not shown).

If we assume the same saturation bound for the *Hes1* protein decay, which is determined by the constant in the numerator of the decay term, in the cytoplasm as in the nucleus, it affects the model only slightly as long as we assure by the choice of the constant in the denominator, that saturation is achieved only in the limit of high concentrations. Taking over the saturation term in the nucleus for the cytoplasmic decay rate without adjusting the denominator, results in a breakdown of the model (data not shown).

3.2. Comparison to biological experiments

Although our model of oscillatory gene expression in the PSM is a broad simplification compared to biological reality it shows some interesting dynamics. An important advantage to other models is the fact that it depends only on short-range signalling and both the ‘clock’ as well as the gradient are formulated as cell-autonomous processes. With this assumption our model can explain experimental findings. For example, Palmeirim et al. (1997) observed ongoing *c-hairy1* oscillation in chick embryos after ablation of parts of the PSM. Later, it was reported that dissection of the PSM in several pieces did not destroy the expression wave (Maroto et al., 2005). We need no simulations for this, because this behaviour follows as a consequence directly from the formulation of the model.

Furthermore, our model explains the independence of embryonic patterning from cell number. Due to enhanced apoptosis the *Aif* mutant mouse embryo consists of only

one tenth of cell numbers of a wild-type embryo at the same developmental stage. Interestingly, both embryos display the same number of somites (Brown et al., 2006). If we halve in our model the growth rate along the PSM and reduce the thickness in the transverse direction accordingly without changing other parameters the distance between expression stripes, measured in cell numbers, halves too (Fig. 2c). The resulting ‘mutant’ PSM consists of one eighth of the cell number of the original PSM, which corresponds to the reduction in cell number observed in the *Aif* mutant.

Another test of the model consists of a simulated over-expression of Fgf8 which is equivalent to changing the coupling of the Fgf8 gradient to the *Hes1* mRNA decay. A fivefold over-expression results in a pattern with very narrow and densely spaced stripes (movie6).

3.3. Delta–Notch coupling synchronisation of PSM cell oscillations

Our above-described model assumes that the division of cells does not affect the oscillator phase, which is of course not realistic. It also disregards the possibility of fluctuations in gene expression, which would destroy the phase coherence between the cellular oscillators (Jiang et al., 2000). Recently, Masamizu et al. provided experimental evidence for cell–cell communication in the PSM as prerequisite for the synchronisation of the *Hes1* oscillator (Masamizu et al., 2006). In zebrafish, Horikawa et al.

(2006) were able to demonstrate that Notch-dependent intercellular communication can facilitate synchronised oscillations. So our aim is to develop a more realistic model in which the newborn cells start with a random phase. Delta–Notch signalling would then synchronise all the oscillating cells in the PSM. Our cell model has methods to recognise nearest neighbours and to create automatically variables for Delta–Notch pairs between neighbouring cells, which are then integrated into the gene regulatory network of each cell. As a first test we generalised Lewis’ Delta–Notch synchronised 2-cell model for *her1/7* oscillations in zebrafish (Lewis, 2003) to a multi-cellular system (Fig. 4). We used the formulas and default parameters given by Lewis in supplement no. 4 to his article. The only differences compared to his model are that we averaged over the Delta-input of the nearest neighbours to reduce boundary effects, and the way we desynchronise the cells when Delta–Notch signalling is not active. Lewis altered the oscillation periods of his cells by diminishing or enhancing the default parameters of the cells by 5%.

In contrast, we do not change the parameters of each cell, but start them with different phases. This is effected by giving each cell (pre-) histories for the *her1/7* protein and mRNA. The (pre-) histories are used when at the start of the simulation the program has to use variables in the delay differential equations where their time-shifted argument would be earlier than the starting point of the simulation. Instead of setting these variables to zero like Lewis did, we cut out a time course from the second half of a pre-recorded oscillation run of one single cell. Its starting point is chosen randomly and its length corresponds to the longest delay in the delay differential equations. Of course, this cannot be done for the Delta-delay. There we follow Lewis in setting all variables with negative time argument to zero.

If one scales up the Delta-delay accordingly, one can use this model also to synchronise *Hes7* oscillators in the PSM of mice using the parameters given in Hirata et al. (2004) (data not shown).

A further (preliminary) result is the following: When the spatial extent of the region and the phase difference between oscillators is too large, different patches of cells are synchronised to different phases of oscillation. These differently synchronised patches can persist side by side for a long time without one taking over the other (data not shown).

Also, it is interesting to note that a Delta-delay that cannot synchronise the oscillations coerces the cellular oscillators into an oscillating ‘salt-and-pepper’ pattern (Fig. 5).

However, the description of the gene expression by delay differential equations is difficult to reconcile with cell division and proliferation because the delays imply a history given for each cell which is certainly different for a newborn and an older cell.

So a model comprising growth and Delta–Notch coupled oscillators requires further work.

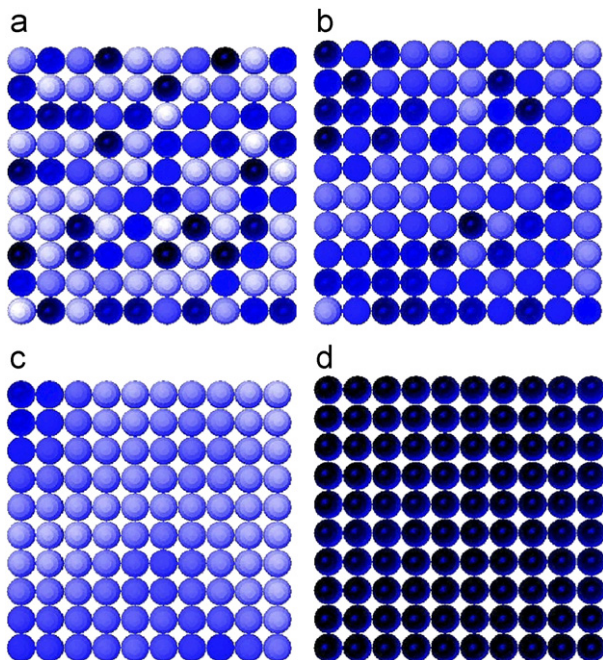


Fig. 4. Synchronisation of *her1* oscillators in a sheet of cell by Delta–Notch signalling shown at three consecutive time points (b–d) after a random start (a). We use the default parameters given in Lewis (2003) supplement no. 4. Here a time delay for the delta protein of 20 min was chosen.

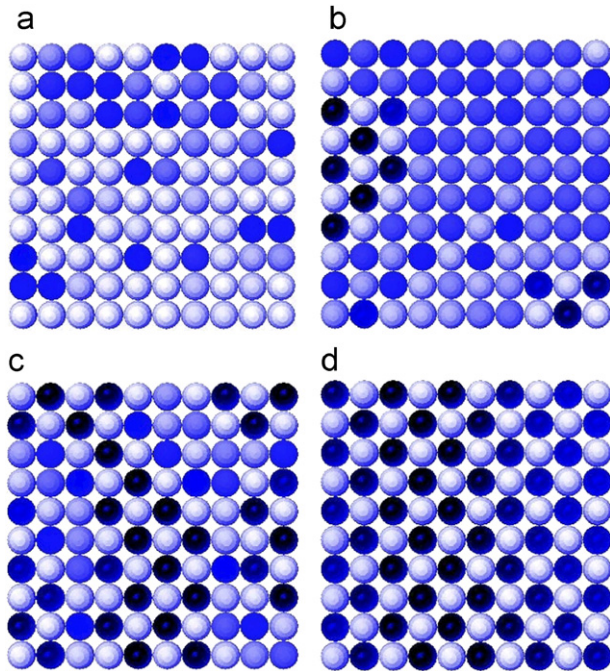


Fig. 5. Failure of synchronisation of *her1* oscillators due to badly chosen Delta-delay producing an oscillating salt-and-pepper pattern. Again we use the default parameter set given in Lewis (2003) supplement no. 4. The only change is a doubled time delay for the delta protein.

4. Discussion

Of course, our model is vastly simplified compared to biological reality. In the following we discuss the various assumptions of the model in more detail and how much evidence from experiment there is:

4.1. Assumptions of the model

To derive these results we had to make the following assumptions:

First of all, we assumed that in each PSM cell a cell-autonomous clock is realised by the *Hes1* oscillator, and that the PSM is growing at its caudal end.

Furthermore, following Dubrulle and Pourquie (2004a), we assumed that only cells in the caudal growth zone express *Fgf8* mRNA. Consequently, a cell-autonomous *Fgf8* mRNA gradient extends from the growth zone, where *Fgf8* is transcribed, into the ‘wave zone’, where *Fgf8* transcription is stopped by an as yet unknown process. There, the mRNA, produced while the cell was located in the growth zone, decays with a half-life which we assumed to be 2 h. This is long compared to the half-lives of *Hes1* mRNA and protein, which have half-lives of approximately 20 min (Hirata et al., 2002). So outside the growth zone only the mRNA which still remains in each cell is being translated into protein.

Finally, we supposed as the simplest approximation that the decay of the *Hes1* mRNA is linearly coupled to the products of Fgf8 signalling. This has the consequence, that

the *Hes1* oscillation period is lengthened ever more as the cell moves away from the growth zone. We disregard the fact, that the *Hes1* mRNA decay rate is probably not only influenced by the Fgf8 signalling, but that there exists a basal mRNA decay (mechanism) which is responsible for the half-life time of long lived mRNAs like *Fgf8* itself.

The Fgf8 gradient could be described only as nearly cell-autonomous because Fgf8 signalling affects the neighbouring cells. In zebrafish endocytosis controls the spreading and effective signalling range of Fgf8 protein, which in this case covers a distance of 10–12 cell diameters in 3 h (Scholpp and Brand, 2004). However, as we assumed the *Fgf8* mRNA gradient to be very shallow, we took the Fgf8 protein in each cell as a measure for the amount of Fgf8 signalling between the cell and its neighbours.

Of course, the linear coupling of the Fgf8 protein to the *Hes1* mRNA decay term hides all intermediate steps of Fgf8 signalling in this simplest possible ‘effective model’. (Here we use the term ‘effective model’ in a way it is used in physics. One assumes that the slow degrees of freedom, i.e. the one with a dynamics which is comparable to the oscillation period determine the dynamics, whereas the ‘fast degrees of freedom’ are ‘integrated out’ and are hidden in the ‘effective constants’.)

The growth zone of our model is only one cell layer thick, because our ‘cells’ cannot move and grow only in the antero-caudal direction if there is free space for the dividing cells (Fig. 2b). In our model each proliferation cycle lasts 9 min. This is certainly a too short generation time, but as the thin growth zone of the model has to stand in for a growth zone which is larger in vivo (Brown et al., 2006), the generation time in our model has to be much shorter than the real one. It follows that our model comprises mainly the ‘wave’ zone of the PSM.

In its present formulation our model comprises only time-dependent processes in each cell. As long as one disregards the spreading of the Fgf8 signal, the only process which determines a spatial scale is the growth rate of the PSM. This consideration may explain the scale invariance of the stripe pattern with respect to varying growth rates, which we mentioned in connection with the *Aif* mutant (Brown et al., 2006).

4.2. Biological evidence supporting our model

It is now generally agreed that the cycling genes *Hes1*, *Hes7* and *Lfng* form an important part of the ‘somitogenesis clock’, possibly with a *Hes7* oscillator working in parallel with others like a *lunatic fringe-Notch1*-oscillator (Bessho and Kageyama, 2003; Bessho et al., 2003). Here we concentrate on *Hes1* because in this case we have the most information to build our model on and *Hes7* seems to work in a very similar way. The role of other cycling genes like *Hes5* and *Hey3* (Kusumi et al., 2004) or *Axin2* (Aulehla and Herrmann, 2004; Aulehla et al., 2003) or *Nkd1* (Ishikawa et al., 2004) is less clear.

There are also various candidates for the gradient of the ‘clock-and-gradient’ model: either *Fgf8* (9, 10) or *Wnt3a* (15, 16) or *Cdx2* (Chawengsaksophak et al., 2004) or *Tbx6* (White and Chapman, 2005)—all emanating from the growing tail-bud. Their decay is, however, not exponentially right to the end. Retinoic acid, originating in the last formed somite, cuts off the tail of the *Fgf8* distribution in the anterior part of the non-segmented PSM. This is not (yet) included in our model.

Although our model is not specific in its choice of *Fgf8* for a ‘cell-autonomous’ gradient coupled to the mRNA decay of *Hes1*, as long as the half-life time of the mRNA forming the gradient is of the order of hours, the following facts are suggestive:

It was found (Delfini et al., 2005) that in the chick “the *Fgf8* gradient is translated into graded activation of the extracellular signal-regulated kinase (ERK) mitogen-activated protein kinase (MAPK) pathway along the PSM”. The MAPK pathway, but also other pathways like Wnt (Briata et al., 2003), is known to influence mRNA stability by controlling mRNA-binding proteins (Baudouin-Legros et al., 2005; Schmidlin et al., 2004). Furthermore, in many cases mRNA stability can be influenced by binding of proteins to the 3’UTR of an mRNA (Wilusz and Wilusz, 2004). In somitogenesis it was discovered that the unusual short half-life of the lunatic fringe mRNA, which shows a similar expression pattern like *Hes7*, depends on the presence of regulatory elements in its 3’UTR, while the much shorter 3’UTR of *Fgf8* mRNA seems to be lacking this elements and has a much longer half-life (Hilgers et al., 2005). In *Xenopus* it was observed (Gautier-Courteille et al., 2004) that the EDEN-BP RNA-binding protein controls the stability of *XSu(H)* mRNA by binding to its 3’UTR and thereby triggering its deadenylation, i.e. poly(A) tail shortening. The *XSu(H)* protein plays a central role in Notch signalling. See also the discussion in the reference mentioned above regarding other cycling genes and human and murine equivalents of EDEN-BP. Finally, Davis et al. (2001) examined the control elements driving the segmental expression of *Xhair2* in *Xenopus* PSM. Its 3’UTR was important for retaining the striped expression pattern. The *Xhair2* 3’UTR could be replaced by the corresponding *Hes1* 3’UTR without changing the expression.

Moreover, the *Hairy2a* 3’UTR confers instability on a heterologous RNA.

Of course, all the circumstantial evidence given above constitutes only clues that maybe our model captures a grain of truth, but certainly constitutes no proof.

4.3. Limitations of the model

At present our model gives only a qualitative correct description of *Hes1* expression:

As mentioned above, the stripe pattern stabilises only asymptotically in time. This is probably a consequence of the fact that the gradient is exponential right to the end of

the PSM, which is certainly not realistic. In vivo a retinoic acid gradient emanating from the formed somites antagonises the *Fgf8* gradient (Dubrulle and Pourquie, 2004b) and so probably provides a cut-off. Also, the neglect of other mRNA decay processes for the *Hes1* mRNA is responsible for the fact, that the stripe pattern persists indefinitely, which is unrealistic, but irrelevant, because certainly other processes come into play after an expression stripe is formed.

Looking at the *Hes1* expression pattern one observes that the anterior and posterior stripe boundaries are not equally sharp defined. In fact, it is hard to decide where one should draw the posterior boundary of expression for a stripe. If one compares this with the old Hirata-model (Hirata et al., 2002) which generates a narrower, more sharply defined expression stripe, but shows similar dynamics, one could surmise that the description of the *Hes1* oscillator on the cellular and molecular level influences the form of the resulting expression pattern. So probably a more realistic description of the cellular processes affecting mRNAs and proteins is called for.

To get a better correspondence between model and reality one should achieve also a more realistic description of the growth zone. There *Fgf8* expression should extent over a larger region of the PSM, new cells should be born in different places, begin their oscillations, and get synchronised by Delta–Notch signalling, before they pass the border to the ‘wave-zone’ where *Fgf8* expression is shut down. Also a more detailed modelling of *Fgf8* signalling would be desirable.

4.4. Concluding remarks

Summarising, we propose that the *Hes1* gene expression ‘wave’ observed in the PSM is a consequence of the fact that the *Hes1* oscillator in each cell slows down ever more as it is moving away from the growing tail-bud. This slow-down results from a corresponding decrease of the *Hes1* mRNA decay rate controlled by a signal transduction pathway which is activated by a gradient of the sort proposed in Dubrulle and Pourquie (2004a).

A similar cell-based model was proposed by Jaeger and Goodwin (2001). However, although they simulated a growing piece of PSM also with object-oriented methods (using C++), their cells contained no gene regulatory network. Instead each cell featured a simple sine function whose period slowed down exponentially with the ‘age’ of each cell.

At the moment quantitative data for modelling somitogenesis are very sparse, but we think our model is flexible enough to incorporate future knowledge about the processes that could be modelled only in a coarse way in this work. Also, although the details of the real gene regulatory network may differ from our simplified model, we think that the mechanism to generate an expression wave like the one for *Hes1* is interesting enough to merit further investigation.

Acknowledgments

We thank Oliver Ehm for performing *Hes1* in situ hybridisations.

S. Zeiser, E. Schneltzer and H.B. Tiedemann were supported by the BFAM project (Bioinformatics for the Functional Analysis of Mammalian Genomes) of the German BMBF.

Appendix A. Supplementary materials

Supplementary data associated with this article can be found in the online version at [doi:10.1016/j.jtbi.2007.05.014](https://doi.org/10.1016/j.jtbi.2007.05.014).

References

- Aulehla, A., Herrmann, B., 2004. Segmentation in vertebrates: clock and gradient finally joined. *Genes Dev.* 18, 2060–2067.
- Aulehla, A., Wehrle, C., Brand-Saberi, B., Kemler, R., Gossler, A., Kanzler, B., Herrmann, B.G., 2003. Wnt3a plays a major role in the segmentation clock controlling somitogenesis. *Dev. Cell* 4, 395–406.
- Baudouin-Legros, M., Hinzpeter, A., Jaulmes, A., Brouillard, F., Costes, B., Fanen, P., Edelman, A., 2005. Cell-specific posttranscriptional regulation of CFTR gene expression via influence of MAPK cascades on 3'UTR part of transcripts. *Am. J. Physiol. Cell Physiol.* 289, C1240–C1250.
- Bessho, Y., Kageyama, R., 2003. Oscillations, clocks and segmentation. *Curr. Opin. Genet. Dev.* 13, 379–384.
- Bessho, Y., Miyoshi, G., Sakata, R., Kageyama, R., 2001a. Hes7: a bHLH-type repressor gene regulated by Notch and expressed in the presomitic mesoderm. *Genes Cells* 6, 175–185.
- Bessho, Y., Sakata, R., Komatsu, S., Shiota, K., Yamada, S., Kageyama, R., 2001b. Dynamic expression and essential functions of Hes7 in somite segmentation. *Genes Dev.* 15, 2642–2647.
- Bessho, Y., Hirata, H., Masamizu, Y., Kageyama, R., 2003. Periodic repression by the bHLH factor Hes7 is an essential mechanism for the somite segmentation clock. *Genes Dev.* 17, 1451–1456.
- Briata, P., Ilengo, C., Corte, G., Moroni, C., Rosenfeld, M.G., Chen, C.Y., Gherzi, R., 2003. The Wnt/beta-catenin → Pitx2 pathway controls the turnover of Pitx2 and other unstable mRNAs. *Mol. Cell* 12, 1201–1211.
- Brown, D., Yu, B.D., Joza, N., Benit, P., Meneses, J., Firpo, M., Rustin, P., Penninger, J.M., Martin, G.R., 2006. Loss of Aif function causes cell death in the mouse embryo, but the temporal progression of patterning is normal. *Proc. Natl. Acad. Sci. USA* 103, 9918–9923.
- Chawengsaksophak, K., de Graaff, W., Rossant, J., Deschamps, J., Beck, F., 2004. Cdx2 is essential for axial elongation in mouse development. *Proc. Natl. Acad. Sci. USA* 101, 7641–7645.
- Cooke, J., Zeeman, E.C., 1976. A clock and wavefront model for control of the number of repeated structures during animal morphogenesis. *J. Theor. Biol.* 58, 455–476.
- Dale, K.J., Pourquie, O., 2000. A clock-work somite. *Bioessays* 22, 72–83.
- Davis, R.L., Turner, D.L., Evans, L.M., Kirschner, M.W., 2001. Molecular targets of vertebrate segmentation: two mechanisms control segmental expression of *Xenopus* hairy2 during somite formation. *Dev. Cell* 1, 553–565.
- Delfini, M.C., Dubrulle, J., Malapert, P., Chal, J., Pourquie, O., 2005. Control of the segmentation process by graded MAPK/ERK activation in the chick embryo. *Proc. Natl. Acad. Sci. USA* 102, 11343–11348.
- Deschamps, J., van Nes, J., 2005. Developmental regulation of the Hox genes during axial morphogenesis in the mouse. *Development* 132, 2931–2942.
- Dubrulle, J., Pourquie, O., 2004a. fgf8 mRNA decay establishes a gradient that couples axial elongation to patterning in the vertebrate embryo. *Nature* 427, 419–422.
- Dubrulle, J., Pourquie, O., 2004b. Coupling segmentation to axis formation. *Development* 131, 5783–5793.
- Gautier-Courteille, C., Le Clainche, C., Barreau, C., Audic, Y., Graindorge, A., Maniey, D., Osborne, H.B., Paillard, L., 2004. EDEN-BP-dependent post-transcriptional regulation of gene expression in *Xenopus* somitic segmentation. *Development* 131, 6107–6117.
- Goodwin, B.C., 1965. Oscillatory behavior in enzymatic control processes. *Adv. Enzyme Regul.* 3, 425–438.
- Hilgers, V., Pourquie, O., Dubrulle, J., 2005. In vivo analysis of mRNA stability using the Tet-Off system in the chicken embryo. *Dev. Biol.* 284, 292–300.
- Hirata, H., Yoshiura, S., Ohtsuka, T., Bessho, Y., Harada, T., Yoshikawa, K., Kageyama, R., 2002. Oscillatory expression of the bHLH factor Hes1 regulated by a negative feedback loop. *Science* 298, 840–843.
- Hirata, H., Bessho, Y., Kokubu, H., Masamizu, Y., Yamada, S., Lewis, J., Kageyama, R., 2004. Instability of Hes7 protein is crucial for the somite segmentation clock. *Nat. Genet.*
- Horikawa, K., Ishimatsu, K., Yoshimoto, E., Kondo, S., Takeda, H., 2006. Noise-resistant and synchronized oscillation of the segmentation clock. *Nature* 441, 719–723.
- Hrabe de Angelis, M., McIntyre II, J., Gossler, A., 1997. Maintenance of somite borders in mice requires the Delta homologue Dll1. *Nature* 386, 717–721.
- Ishikawa, A., Kitajima, S., Takahashi, Y., Kokubo, H., Kanno, J., Inoue, T., Saga, Y., 2004. Mouse Nkd1, a Wnt antagonist, exhibits oscillatory gene expression in the PSM under the control of Notch signaling. *Mech. Dev.* 121, 1443–1453.
- Jaeger, J., Goodwin, B.C., 2001. A cellular oscillator model for periodic pattern formation. *J. Theor. Biol.* 213, 171–181.
- Jiang, Y.J., Aerne, B.L., Smithers, L., Haddon, C., Ish-Horowicz, D., Lewis, J., 2000. Notch signalling and the synchronization of the somite segmentation clock. *Nature* 408, 475–479.
- Jouve, C., Palmeirim, I., Henrique, D., Beckers, J., Gossler, A., Ish-Horowicz, D., Pourquie, O., 2000. Notch signalling is required for cyclic expression of the hairy-like gene HES1 in the presomitic mesoderm. *Development* 127, 1421–1429.
- Koonin, S.E., 1986. *Computational Physics*. Addison-Wesley Pub. Co., Menlo Park, CA.
- Kusumi, K., Mimoto, M.S., Covello, K.L., Beddington, R., Krumlauf, R., Dunwoodie, S.L., 2004. Dll3 pudgy mutation differentially disrupts dynamic expression of somite genes. *Genesis* 39, 115–121.
- Lewis, J., 2003. Autoinhibition with transcriptional delay: a simple mechanism for the zebrafish somitogenesis oscillator. *Curr. Biol.* 13, 1398–1408.
- Maroto, M., Dale, J.K., Dequeant, M.L., Petit, A.C., Pourquie, O., 2005. Synchronised cycling gene oscillations in presomitic mesoderm cells require cell–cell contact. *Int. J. Dev. Biol.* 49, 309–315.
- Masamizu, Y., Ohtsuka, T., Takashima, Y., Nagahara, H., Takenaka, Y., Yoshikawa, K., Okamura, H., Kageyama, R., 2006. Real-time imaging of the somite segmentation clock: revelation of unstable oscillators in the individual presomitic mesoderm cells. *Proc. Natl. Acad. Sci. USA* 103, 1313–1318.
- Monk, N.A., 2003. Oscillatory expression of Hes1, p53, and NF-kappaB driven by transcriptional time delays. *Curr. Biol.* 13, 1409–1413.
- Muratani, M., Tansey, W.P., 2003. How the ubiquitin–proteasome system controls transcription. *Nat. Rev. Mol. Cell Biol.* 4, 192–201.
- Murray, J.D., 2002. *Mathematical Biology*. Springer, New York.
- Palmeirim, I., Henrique, D., Ish-Horowicz, D., Pourquie, O., 1997. Avian hairy gene expression identifies a molecular clock linked to vertebrate segmentation and somitogenesis. *Cell* 91, 639–648.
- Rivett, A.J., 1998. Intracellular distribution of proteasomes. *Curr. Opin. Immunol.* 10, 110–114.

- Saga, Y., Takeda, H., 2001. The making of the somite: molecular events in vertebrate segmentation. *Nat. Rev. Genet.* 2, 835–845.
- Schmidlin, M., Lu, M., Leuenberger, S.A., Stoecklin, G., Mallaun, M., Gross, B., Gherzi, R., Hess, D., Hemmings, B.A., Moroni, C., 2004. The ARE-dependent mRNA-destabilizing activity of BRF1 is regulated by protein kinase B. *EMBO J.* 23, 4760–4769.
- Scholpp, S., Brand, M., 2004. Endocytosis controls spreading and effective signaling range of Fgf8 protein. *Curr. Biol.* 14, 1834–1841.
- Takebayashi, K., Sasai, Y., Sakai, Y., Watanabe, T., Nakanishi, S., Kageyama, R., 1994. Structure, chromosomal locus, and promoter analysis of the gene encoding the mouse helix-loop-helix factor HES-1. Negative autoregulation through the multiple N box elements. *J. Biol. Chem.* 269, 5150–5156.
- White, P.H., Chapman, D.L., 2005. Dll1 is a downstream target of Tbx6 in the paraxial mesoderm. *Genesis* 42, 193–202.
- Wilusz, C.J., Wilusz, J., 2004. Bringing the role of mRNA decay in the control of gene expression into focus. *Trends Genet.* 20, 491–497.
- Zeiser, S., Müller, J., Liebscher, V. Modelling the Hes 1 oscillator. *J. Comput. Biol.*, in press.